AKADÉMIAI KIADÓ

UNIVERSITY of DEBRECEN

International Review of Applied Sciences and Engineering

14 (2023) 2, 201–211

DOI:
10.1556/1848.2022.00494

ORIGINAL RESEARCH PAPER

Simulation aided design of a high efficient GaSb based single-junction solar cell

Fatima Zahra Kharchich* and Abdellatif Khamlichi

[1] Systems of Communication and Detection Laboratory, ENSA Tetouan, University Abdelmalek Essaadi, 93002, Tetouan, Morocco

Received: March 16, 2022 • Accepted: July 10, 2022
Published online: January 10, 2023

ABSTRACT

Owing to their elevated absorption coefficient, superior resistance to radiation and reduced effective electron mass, gallium antimonide (GaSb) semiconductors were documented to be suitable for photovoltaic systems applications. However, they were found to suffer from low efficiency. This work has been dedicated to enhance the design of GaSb based single-junction solar cells having window and back surface field made from AlGaAsSb material. The purpose is to maximize their electrical performance by considering doping and thickness of layers as design variables. A methodology of optimization was proposed. It is based on computer aided design through simulations performed under SILVACO-ATLAS software and a numerical procedure that was developed to achieve optimal design of this particular solar cell. The approach encompasses analysis of variance and derivation of response surface models to get explicit expression of the objective function corresponding to efficiency. The obtained results have shown an efficiency which is higher than all the previous known values established in literature.

KEYWORDS

GaSb solar cells, technology computer aided design, SILVACO-ATLAS, response surface modelling, optimization, efficiency

1. INTRODUCTION

Due to their versatile applications, the antimonide based materials, particularly gallium antimonide (GaSb) semiconductors, attract currently renewed scientific interest. GaSb belongs to the III-V binary semiconductor compounds. It is characterised by a direct bandgap of 0.72 eV and a long wavelength infrared response which extends to 1800 nm. These properties enable GaSb material to be suitable for high-speed near-infrared application [1]. The GaSb semiconductor shows also a reduced dependency to temperature, and good refractive index and dielectric constant, which have made it attractive in the field of optoelectronic devices [2]. Because of its elevated absorption coefficient, superior resistance to radiation and reduced effective electron mass, GaSb was recognized also to be a good semiconductor material for thermophotovoltaics systems applications [3].

The first GaSb photovoltaic cell was fabricated in 1989. Then this single cell was used as a booster cell under GaAs material in a mechanically stacked structure, for space satellite applications. This GaAs/GaSb tandem combination has yielded an efficiency of 31% under concentration [4]. Later, by using a simple Metal Organic Chemical Vapor Phase Deposition (MOCVD) method, a dual GaAs/GaSb cell with double layer of antireflection coating has demonstrated an efficiency of 31.1% under 100 × AM1.5d irradiation conditions [5]. Despite these attainments, GaAs/GaSb tandem solar cells have been documented to suffer from low open circuit voltage. This is because of the observed large lattice mismatch between GaSb based structure and GaAs material used as substrate. Interfacial misfit dislocations occur at the surface separating the substrate from the device structure. These defects propagate into the active region of the heterostructure causing limitation of performance. To reduce

*Corresponding author.
E-mail: kharchichfatima@gmail.com

AKJournals

the lattice mismatch problem encountered in GaSb based structures, various solutions were proposed. These include the use of defect filter consisting of a thin InGaSb, InGaP or AlSb buffer layer in order to release strains appearing during the growing process, which are responsible for misfit dislocations. This was proved to be successful in the case of the InGaP/GaSb dual junction [6]. The work has reported an efficiency and open circuit voltage of, respectively, 44.05% and 2.66 V under 1000 suns for the AM1.5G spectrum.

To grow GaSb-based heterostructures, many of the well known epitaxial techniques can be employed. These include liquid-phase epitaxy, molecular beam epitaxy and organometallic vapor-phase epitaxy [7]. GaSb material is lattice matched to numerous III-V ternary and quaternary compounds, like InGaAsSb and AlGaSb. This has motivated researchers to carry out trials on the suitability of GaSb as a sub cell in multi-junction solar cells. The first experimental result of a wafer bonded four junction solar cell based on GaSb has reached an efficiency of 29.1% at 194 suns [8]. Subsequently, a 4-terminal obtained by mechanical stacking according to the following architecture GaInP/GaAs/GaInNAsSb/GaSb/GaInAsSb has been realised [9]. It has reached an efficiency of 44.5%. Thereby, conversion efficiency beyond 50% has been expected for such combined cascaded cells [10]. To complete this, persistent actions are needed to fully explore the possibility of achieving higher efficiencies.

The production, testing and optimization process of multi-junction solar cells are exorbitant and onerous in practice. This is because the processes should be repeated many times till the desired results are obtained. As the tendency is moving continually towards the miniaturization of devices and many factors can intervene for a given device configuration, it becomes difficult to investigate all the physical processes experimentally. So, simulation is needed in this framework. It enables investigating parametrically the characteristics of a given architecture or exploring new original ones. This simulation based approach is employed in the present work. Based on a recent experimental work [11], the chosen structure of the single-junction solar cell which will be studied here comprises a GaSb Base and Emitter layers sandwiched between lattices corresponding to $Al_{0.5}Ga_{0.5}As_{0.04}Sb_{0.96}$ Back Surface Field (BSF) and Window layers. It was reported earlier that the AlGaAsSb quaternary alloys are a good choice for the Window layer as they cover the visible and infrared parts of the spectrum (0.57–1.72 μm) [12].

The simulations which are carried out in the following are performed by using two tools: the 2D SILVACO-ATLAS software and analysis of variance of data results performed on the considered intervals used in parametric studies. A process of optimisation which consists of three steps is then proposed in order to determine the best design with regards to efficiency of the selected architecture of GaSb based single junction solar cell. The above mentioned software offers the possibility to conduct parametric simulations in order to analyse, with good accuracy, the effect of various design variables on the performance of different semiconductor devices [13]. It allows also investigating the effect of manufacturing tolerance on performance. This last feature makes it possible to achieve a proper balance between manufacturing and design based on simulation [14].

The objective of this work is to determine optimal design of a GaSb based single-junction solar cell fitted with window and BSF thin layers made from $Al_{0.5}Ga_{0.5}As_{0.04}Sb_{0.96}$. The optimization procedure will be conducted on practical ranges of parameters in order to make the device realizable in practice. These ranges are fixed based on recent experimental work performed on a solar cell having the same investigated architecture. The proposed optimisation process targets to achieve optimal efficiency for the studied solar cell structure by considering all the significant factors which include layers thicknesses and their doping. Contrary to the usual methods, the proposed optimisation process has the capacity of reaching with reasonable computational cost an optimal design for which the efficiency is higher than those published previously in the literature.

This paper is organized as follows. In section 2, a description of the simulation framework used to predict performance of the studied solar cell is given. This presents the main features of the physically-based solar software packages used in the present study, as well as the related physical models. Then, the procedure of carrying out a solar cell simulation under this finite element environment is presented, along with the solar cell material input parameters that are assumed in this work. The next section provides a concise description of the numerical procedure developed for achieving global optimization of the considered structure. A comparison of the obtained results with prior experimental and theoretical works is finally given, before summing up the main conclusions of the work and outlining future perspectives.

2. SIMULATION OF SOLAR CELLS UNDER SILVACO-ATLAS SOFTWARE

2.1. Software description

In this study, SILVACO-ATLAS Software (Deck Editor Version 4.2.5.R) was used for the numerical simulation of the single-junction Gasb solar cell. This software is a physically based solar simulator tool that has been developed by SILVACO International [15]. It is based on the finite element method and enables to predict the electrical and optical characteristics of defined semiconductor structures. To enable that, this numerical tool solves fundamental physical equations using Newton coupled and Gummel decoupled methods through a two dimensional grid. These equations are derived from those of Maxwell and include Poisson's, continuity and transport equations [16]. For the description of physical mechanisms, the software offers varied choices of physical models. They are specified by the user and belong to either one of the following five models: description of mobilities, recombination rate, carrier statistics, ionization and tunnelling.

The mobility enables to fix the drift velocity of carriers as being proportional to the electric field. For common solar cells, this property appears to be independent from the intensity of the electric field. Mobility is due to scattering resulting from lattice phonons and impurity induced mechanisms. It depends on temperature and doping and decreases with impurity concentration. Empirical models are used in practice to predict carrier mobilities.

Recombination is a process by which an illuminated semiconductor tends to recover a state of equilibrium. The electron and hole concentrations relax by falling from conduction bands to valence bands. There exist three main mechanisms which occur in parallel and yield recombination: presence of defects in the forbidden gap (Shockley-Read-Hall), radiation from band to band, and radiation according to Auger mechanism, in which energy is offered to another carrier before this last relaxes thermally through phonons. Physical models have been developed and can be used to predict the actual recombination rate.

In semiconductors, the carriers of currents consist of both electrons and holes. In an equilibrium state, the densities of these carriers can be predicted by means of the Fermi - Dirac statistics. In this context, the concept of Fermi energy plays a fundamental role. This energy can be estimated under the quasineutrality assumption; it lays close to that of the band gap middle in clean crystals and approaches the energy of an impurity in case of doped materials. According to Boltzmann, the activation energy is associated to the difference existing between a band edge and a Fermi level. The product of the activation energy with the density of energy states gives then the carrier density.

Impact ionisation corresponds to transfer of energy to an electron by optical absorption. This causes the bond of the electron with an atom of crystal to break. A pair of electron and hole is then created. Tunnelling current is associated to the probability that exists for an electron, in a semiconductor, to be directly excited from a valence band to a conduction band. This phenomenon occurs when a sufficiently intensive electric field is present and can be local or non-local. Various probability equations are available for predicting tunnelling such as the Wentzel-Kramers-Brillouin method.

Depending on the nature of materials composing the studied solar cell, the user has to specify the appropriate models to be used in simulation. This can be done for a layer or the entire cell structure. Selection of the adequate models depends on many parameters such as doping level, intensity of fields.

Accuracy of simulations depends hugely on the basic physical models that are declared. So, the user should fix them at first by considering comparison with previously works or by verifying predictions with available experimental results. In the present work, this important phase of models checking will be performed in the next section.

2.2. Structure and material properties of the considered solar cell

The reference structure design of the GaSb single-junction solar cell which is considered in this work is schematically represented in Fig. 1. This device architecture was selected

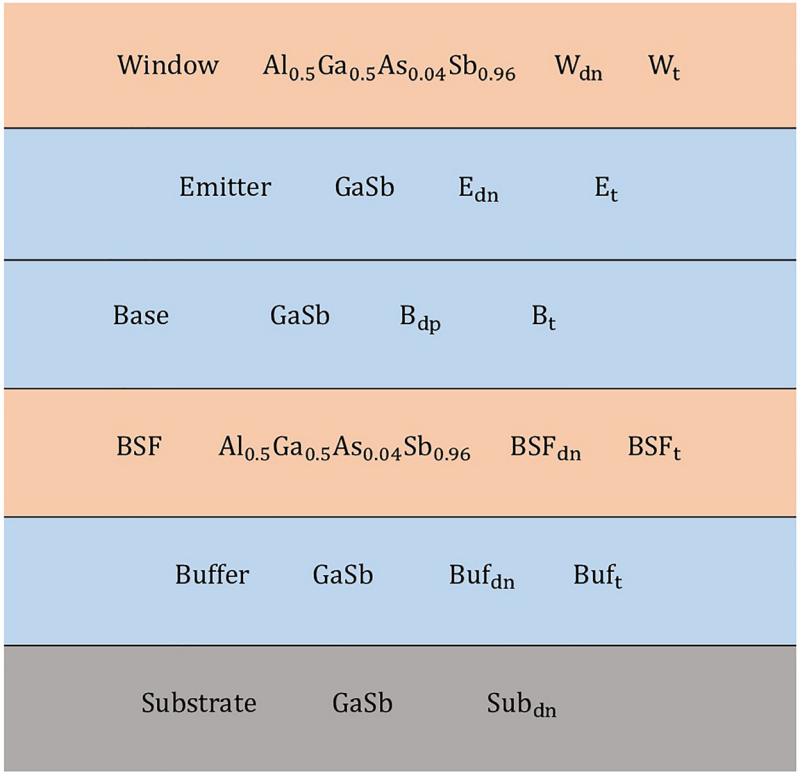

Fig. 1. The studied structure of the GaSb single-junction solar cell having window and BSF filter layers as depicted. (Own source)

based on the experimental work described in [10–11]. It is formed from bottom to top by a 200 nm thick GaSb buffer doped negatively and deposited on an n-type substrate. The buffer is roofed by an n-type AlGaAsSb BSF with a carrier concentration of $1.5\times10^{18}\ cm^{-3}$ and thickness of 25 nm. This is followed successively by a 3 μm thick n-type Base layer with concentration $10^{17}\ cm^{-3}$, and a p-type Emitter having 100 nm of thickness and carrier concentration of $10^{19}\ cm^{-3}$. Finally, the whole is sheltered by a wide band gap p-doped AlGaAsSb Window layer having 10 nm of thickness and $3\times10^{19}\ cm^{-3}$ of carrier concentration.

Table 1 gives the material parameters that are used in this work. They have been taken from the following literature research and experimental work [11, 15, 17]. The numerical simulations were carried out under 1 sun, at temperature 300 K and for AM 1.5G spectral condition matching the ASTM standard spectra.

The standard conditions were introduced in order to be able to compare universally performance of solar cells. They include spectrum, light intensity and temperature. The prefix AM (which is an acronym for Air Mass) is used as reference to the sunlight standard spectrum. It is followed by a number indicating the length of the light ray path through the terrestrial atmosphere. This number fixes the available energy distribution of sunlight at the surface of earth in generic locations. Measured solar cell characteristics are usually given for an air mass equal to 1.5, which is associated to sun having the zenith angle of 48.19°s. The AM1.5 global spectrum, which is denoted AM1.5G, is considered in the particular conditions of flat plate photovoltaic modules under the light irradiance power density of 1 kW/m^2. The standard test conditions correspond to a cell temperature of 300 K and AM1.5G spectrum. The sunlight intensity can be increased through concentration. The obtained light intensity is then designated as a multiple of one sun which is associated to flat conditions with the unit power density of 1 kW/m^2. Here, the solar cell is assumed to operate under 1 sun conditions.

Before performing simulations which are specific to the subject of the present work, a preliminary simulation was executed for the purpose of validation of the software outcome with regards the physical models and mesh to be used. This consisted of a comparison between the performance of the experimental cell studied in [11] and that which is predicted through numerical simulation performed on the same device. The obtained results are given in Table 2. The comparison shows that the experimental and simulated characteristics are enough close one to each other. So, the accuracy of the outputs of the software used here can be thought of to be reliable to an acceptable level of confidence regarding the afterward simulations.

Further details about the physical models used and meshing of the cell structure are given in the subsequent section.

Table 1. Material parameters of the studied solar cell (at 300 K). (Own source)

Material parameter	GaSb	$Al_{0.5}Ga_{0.5}As_{0.04}Sb_{0.96}$
Band gap $E_g(eV)$	0.726	1.35
Lattice constant (Å)	6.096	6.096
Electron affinity (eV)	4.09	3.83
Relative permittivity ε_r	15.7	13.8
h^+ mobility $(cm^2\cdot V^{-1}\cdot S^{-1})$	15	530
e^- mobility $(cm^2\cdot V^{-1}\cdot S^{-1})$	15	200
Radiative recombination rate $(cm^3\cdot S^{-1})$	8.5×10^{-11}	8.5×10^{-11}
Electron, Hole Auger coefficient $(cm^6\cdot S^{-1})$	5×10^{-30}	5×10^{-30}

2.3. Physical models

The numerical modelling approach is based on the drift-diffusion model that has been largely used in simulations dedicated to the transport phenomenon over hetero-interfaces. This relays on the assumption that quasi-Fermi levels are continuous at the heterojunctions interfaces. The drift-diffusion approximation is based on the Boltzmann transport theory which was found to hold for almost all practical devices [15]. According to this modelling, the current densities can be given explicitly in terms of the quasi-Fermi levels under the following form:

$$\overrightarrow{J_n} = -q\mu_n \times n\overrightarrow{\nabla}\phi_n \tag{1}$$

$$\overrightarrow{J_p} = -q\mu_p \times p\overrightarrow{\nabla}\phi_p \tag{2}$$

where q is the elementary charge, ϕ_n, respectively ϕ_p, is the quasi-Fermi level associated to electrons, respectively to holes, μ_n and μ_p are the associated mobilities of carriers and $\overrightarrow{\nabla}$ is the nabla symbol.

Using the Boltzmann approximation, the quasi-Fermi levels can be related to the potential and carrier concentrations as follows:

$$n = n_{ie}\exp\left[\frac{q(\Psi-\phi_n)}{k\ T_L}\right] \tag{3}$$

$$p = n_{ie}\exp\left[\frac{-q\left(\Psi-\phi_p\right)}{k\ T_L}\right] \tag{4}$$

where n and p are respectively the carrier densities of electrons and holes, n_{ie} is the effective intrinsic concentration, k the Boltzmann constant, Ψ the intrinsic potential and T_L the lattice temperature.

Table 2. Comparison between the electrical parameters of GaSb solar cell as obtained from experiment and simulation. (Own source)

Nature of the work	V_{oc} in V	J_{SC} in mA/cm^2	FF in %	Efficiency in %
Experiment [11]	0.312	38.80	59.60	7.26
Simulation	0.319	38.80	62.07	7.26

Eqs. (4) and (5) can be inverted to give the quasi-Fermi potentials as:

$$\phi_n = \Psi - \frac{k\ T_L}{q} \ln\left(\frac{n}{n_{ie}}\right) \tag{5}$$

$$\phi_p = \Psi + \frac{k\ T_L}{q} \ln\left(\frac{p}{n_{ie}}\right) \tag{6}$$

To the previous equations one should add the continuity equations and the Poisson's equation which take the following form

$$\frac{\partial n}{\partial t} = g + \frac{1}{q}\nabla.\overrightarrow{J}_n \tag{7}$$

$$\frac{\partial p}{\partial t} = -g - \frac{1}{q}\nabla.\overrightarrow{J}_p \tag{8}$$

$$\overrightarrow{\nabla}.\left(\varepsilon\overrightarrow{\nabla}\psi\right) = -q\left(p - n + N_D^+ - N_A^-\right) \tag{9}$$

where g regroups the net generation and recombination rates of electrons, ε is the static permittivity of the medium, N_A^-, respectively N_D^+, is the concentration of ionized acceptors impurities, respectively that of donors impurities.

The net carrier generation-recombination rate g takes into account mechanism related to defects, and impact and avalanche ionization. This rate can be correlated to the field variables $n, p, \psi, \mu_n, \mu_p, \phi_n, \phi_p$ of well-known physical models such as that of Shockley-Read-Hall which enables predicting the effect due to defects. For a given solar cell structure, the model equations along with the constitutive relations and boundary conditions can be solved by means of the finite element method. It should be noticed that a key step in this process of solution is specifying an adequate mesh. Accuracy of solution will be affected by the mesh used if mesh-convergence is not yet stated. This is a fundamental issue to deal with in the context of the finite element method. When building a mesh, one should always adapt it in order to get accurate solution of the considered equations.

In the present case, a 2D approximation of the problem is assumed and the mesh is constituted by triangular elements with the solution determined at the intersection edge nodes. It is well known that working with a finer mesh is better. But, this yields a large number of algebraic equations to be solved. Even if theoretically the expected resolution is higher, from a numerical point of view the number of equations is large and the required run time for their inversion could be excessive. Furthermore, numerical instabilities could occur if the system is sparse. On the opposite, if the mesh is coarser, resolution decreases as well as the run time. To successfully set an adequate mesh, one should equilibrate these antagonistic effects. This could be achieved by recognizing at first where gradients of the solution are predominant. In our case, the strong variations occur in the junctions of N+N or N+P type. So, in these zones a finer mesh is required in order to retrieve accurately the spatial changes of the solution. With a coarser mesh, the solution will suffer from loss of information in these vital areas of the solar cell domain. Through performing sufficient numerical trials, the optimal mesh can be fixed to ensure convergence of the solution, with negligible discretization errors and minimum run time.

In the particular case of the software used for simulations in this study, the total number of nodes is limited to 100 k. This was found to be sufficient for the discretization of our problem. The software provides an automatic interface that enables a user to build the mesh structure. This interface uses the information about the materials assigned to the cell structure and detects the direction of main current. If this last corresponds to the y direction, the user can indicate only the position of mesh lines in the x direction. Those parallel to y-axis are then automatically determined based on the specified regions of the cell structure.

In the performed simulations, the results were found to be almost insensitive to the number of x lines used for meshing, because the problem is predominantly 1D in the y direction. No significant changes affect the output results if the number of x lines is increased beyond 18. The critical areas of GaSb and AlGaAsSb heterojunctions have been discretised automatically with a finer spacing in the y-direction that enables to capture correctly the underlying physics. Figure 2 shows the mesh used in simulations which enables to ensure both convergence of the solution and minimum run time.

3. NUMERICAL PROCEDURE FOR OPTIMIZING THE GASB SINGLE-JUNCTION SOLAR CELL

One can understand easily that performance of the GaSb single-junction solar cell with AlGaAsSb window and BSF layers varies as function of the geometric and materials properties of the cell strucutre. These include thickness and doping of the differtent layers composing the structure of the solar cell which are termed in the following design variables. The nomenclature and units of parameters used as input design variables are given in Table 3. Optimization of an objective function considered as the output of interest in design consists then in finding the values of design variables that achieve optimal value of this function. Many approaches can be considered to solve this mathematical program and various procedures have been proposed in the literature. However, simplicity, robustness and computational time constitute main features that are of concern to the practitioners.

In this work focus is on efficiency of a solar cell. A numerical procedure is proposed in order to find the optimal design with regards to efficiency for the particular structure of solar cell depicted in Fig. 1. The approach starts with the initial design of the solar cell that was experimentally tested as given in [11]. Then evaluation of the relative influence of parameters, which were centered on the previous design values, on solar cell performance is performed through analysis of variance. This allows determining the parameters that have the most influence on the efficiency in order to retain them in the

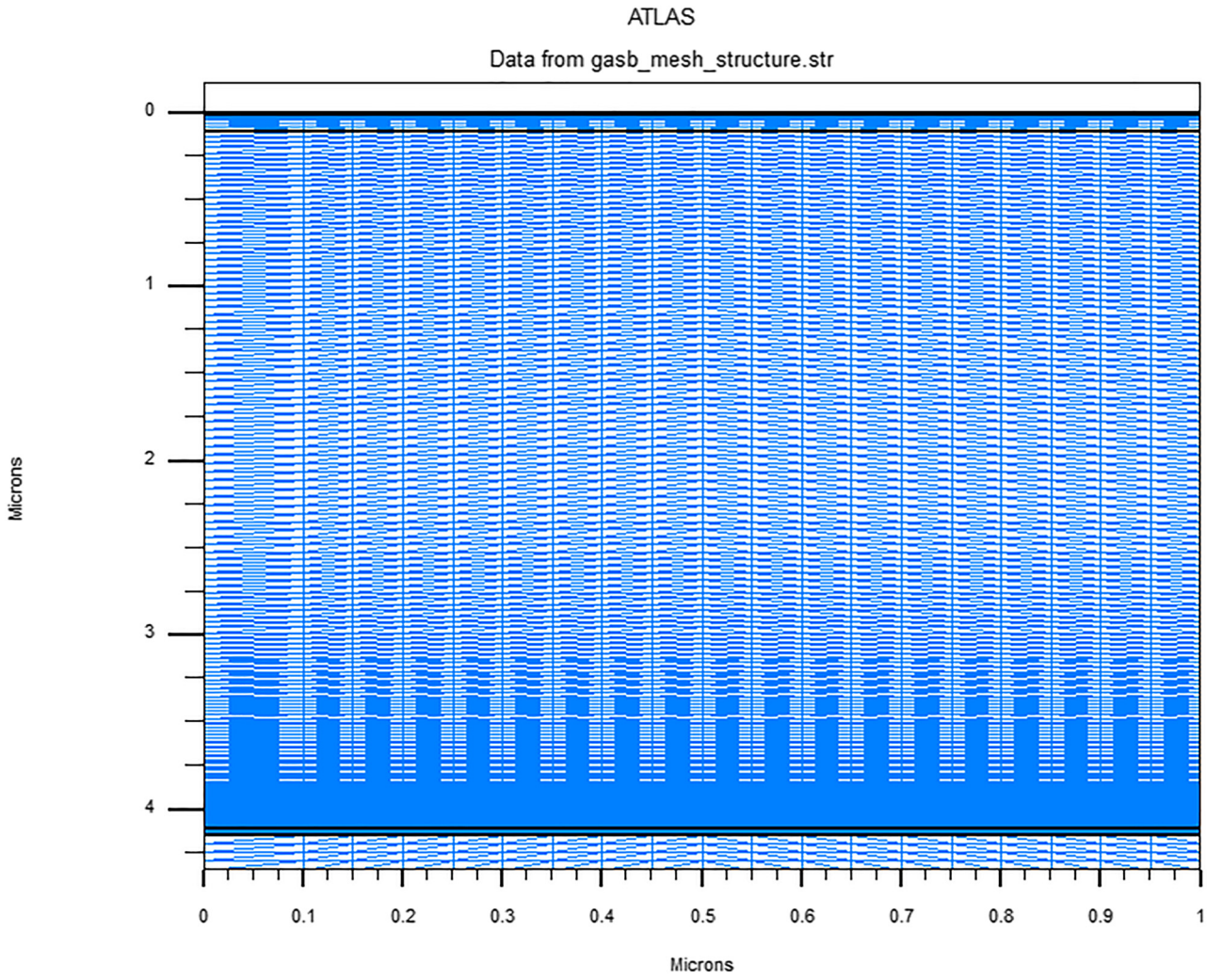

Fig. 2. Solar cell mesh model enabling convergence of the calculated solution. (Own source)

Table 3. Ranges of design variables considered in the optimization procedure of GaSb single-junction solar cell with AlGaAsSb window layer. (Own source)

Parameter	Unit	Symbol	Low bound	Upper bound
Window doping	cm^{-3}	*Wd*	3×10^{18}	3×10^{20}
Window thickness	μm	*Wt*	0.01	0.01
Emitter doping	cm^{-3}	*Ed*	10^{18}	10^{20}
Emitter thickness	μm	*Et*	0.08	0.2
Base doping	cm^{-3}	*Bd*	10^{16}	10^{18}
Base thickness	μm	*Bt*	2	4
BSF doping	cm^{-3}	*BSFd*	1.5×10^{17}	1.5×10^{19}
BSF thickness	μm	*BSFt*	0.015	0.035

subsequent steps of the optimization process. Following selection of the relevant design variables, the physically based simulation is performed according to a full factorial design table constructed on these variables. The design variables were varied according to either two or three levels, depending on whether variability of efficiency is considered alone or finer representation of the efficiency is desired. Based on the obtained results of simulations, meta-modelling is then performed to obtain a surface response model. This is provided by using regression tools under MATLAB software to obtain explicit expression of the simulation outcomes in terms of the design variables. Depending on the obtained value of the determination coefficient R^2, through using the command *regress*, a linear or a quadratic polynomial is determined. The obtained response surface model serves then to determine the optimal combination of design variables by solution of a constrained mathematical program where use is made of the command *fmincon*.

One should notice that the proposed optimization method enables to limit to a strict minimum the number of simulations. In fact, the total number of simulations based on a primitive full factorial design of experiment table including all the eight factors given in Table 3, with three levels selected for each one of them, would require a total number of $3^8 = 6561$ simulations. This is too large to achieve in practice with reasonable time and effort. The proposed procedure in this work is simpler and allows for reaching an optimum design with more affordable run time. It consists of the three steps that are explicated in the following.

3.1. Preliminary simulations

The objective of the preliminary simulations is to guess variability of the efficiency as function of the design variables within their ranges as specified in Table 3. This enables to identify the factors which have the largely effect on efficiency of the solar cell. A series of simulations were carried out according to a full factorial table based on two levels for each variable: the lower bound and the upper bound that are indicated in Table 3. According to early simulations, changing the Window thickness would not affect the solar cell efficiency as long as the thickness value exceeds the threshold of 0.01 μm. Except then from the Window thickness which was fixed at $Wt = 0.01\ \mu m$, all the other variables were considered to be active in the analysis of variance. The simulation layout plan included a total number of $2^7 = 182$ combinations.

Figure 3 gives the obtained efficiency as function of the combination number. The combinations are defined by a full factorial table constructed in a conventional way on data given in Table 3. The highest value of efficiency reached is $\eta = 10.60\%$.

Analysis of variance was performed on the obtained results by using a first order model through the MATLAB command *anovan*. The obtained relative influence of factors in the considered intervals is as follows: *Wd* (40.8%), *Et* (21.04%), *Ed* (11.8%), *Bd* (4.05%). It was found also that the three other factors contribute together to variability of efficiency with less than 2.7%. These results signify that variability of efficiency is mainly dominated by Window doping as well as Emitter thickness. These are followed by Emitter doping and Base doping, while the other factors have negligible effect on efficiency. Note that there exists a part of hidden variability 19.6% which is not explicitly explained by the considered factors through the linear regression model used here. However, this has no effect on significance of the obtained results as it will be seen in the next section by considering a more accurate quadratic regression model. Taking into account the results offered by the preliminary simulations, the least influential design parameters were fixed at the following values: $Bt = 4\mu m$, $BSFd = 1.5\times19^{19} cm^{-3}$ and $BSFt = 0.035\mu m$.

3.2. Second series of simulations

A second series of simulations was performed in order to assess more closely dependency of the solar cell outputs versus the four dominant factors obtained in section 3.1. For this purpose, three levels have been chosen for each factor. Note that from results of the previous section, it was found that efficiency increases with Window doping and Base doping, so the intervals containing these factors were centered on their upper bounds, respectively, $3\times10^{20} cm^{-3}$ and $10^{18} cm^{-3}$. It was found also that efficiency decreases with Emitter doping and Emitter thickness, these last factors were then centered on their lower bounds, which are respectively, $10^{18}\ cm^{-3}$ and 0.08 μm. Table 4 gives the three levels selected for the most influential factors as considered in this new series of simulations. The simulation layout plan included then a total number of $3^4 = 81$ combinations.

Figure 4 gives the obtained efficiency as function of the combination number. These are defined according to a full factorial table which is constructed in a conventional way on data of Table 4. The obtained highest value of efficiency is $\eta = 10.94\%$.

Table 4. Levels of the parameters considered in the second series of simulations. (Own source)

Factor	$Wd(cm^{-3})$	$Ed(cm^{-3})$	$Et(\mu m)$	$Bd(cm^{-3})$
Low level	10^{20}	5×10^{17}	0.06	5×10^{17}
Intermediate level	3×10^{20}	10^{18}	0.08	10^{18}
High level	5×10^{20}	1.5×10^{18}	0.1	1.5×10^{18}

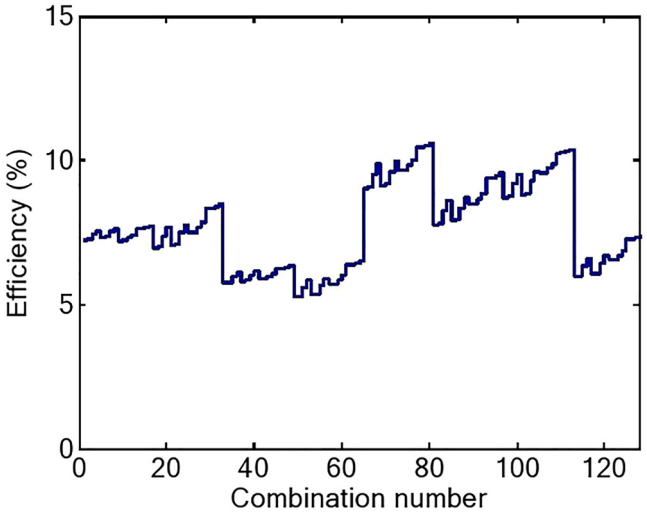

Fig. 3. Efficiency of GaSb solar cell versus the combination number for the considered parameters with their two levels as given in Table 3. (Own source)

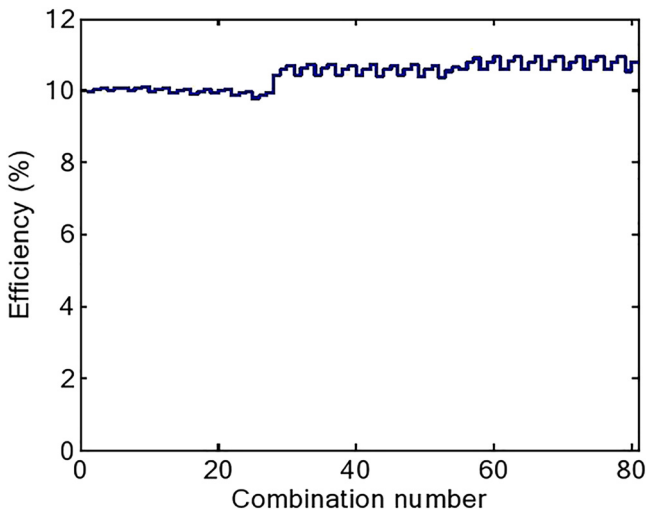

Fig. 4. Efficiency of GaSb solar cell versus the combination number for the considered parameters with their three levels as given in Table 4. (Own source)

The results of simulations were processed to perform analysis of variance in the considered intervals of factors that are specified in Table 4. By using a quadratic regression model, this resulted in the following values of influences: *d* (89.64%), *Bd* (7.94%), *Wd*×*Bd* (1.24%), *Et* (0.3%) and other (0.2%). Note that the influences have changed in comparison with those corresponding to section 3.1, because the intervals have changed and their lengths have been reduced here in order to increase the value of the coefficient of determination. The R^2 value reaches 99.7%, while it was just 80.4% in the previous section where only linear regression was performed. So, to a high level of confidence, the dominant factors are Window doping and Base doping as well as their interaction. It was found that efficiency increases with increasing values of these two factors. As a conclusion of these second series of simulations, only Window doping and Base doping will be considered in supplementary simulations in order to improve further the design of solar cell structure. The other less influential factors are fixed as follows: $Bt = 4\ \mu m$, $BSFd = 1.5\times10^{19}\ cm^{-3}$, $BSFt = 0.035\ \mu m$, $Ed = 5\times10^{17}\ cm^{-3}$ and $Et = 0.1\ \mu m$.

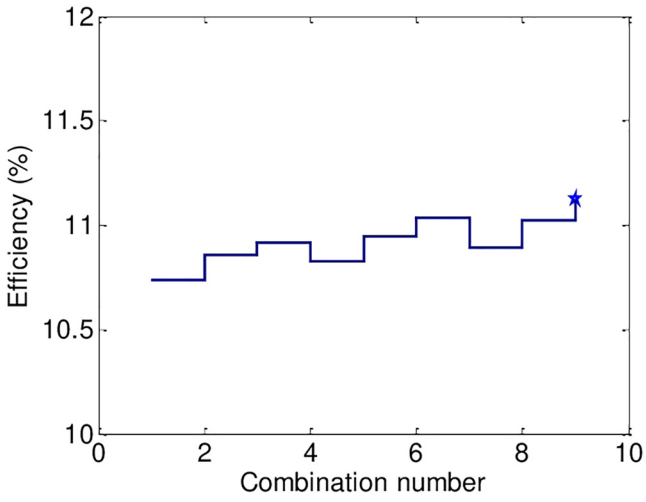

Fig. 5. Efficiency of GaSb solar cell versus the combination number for the considered parameters with their three levels as given in Table 5, the star represents the best efficiency. (Own source)

3.3. Third series of simulations

In this final series of simulations, the dominant factors Wd and Bd are varied according to the levels fixed in Table 5. The ranges of intervals containing these factors were increased. This is because, as stated in section 3.2, efficiency increases with the values of Wd and Bd.

Based on Table 5, a full factorial table consisting of $3^3 = 9$ combinations was constructed. The obtained efficiency results from simulations are plotted in Fig. 5. It can be seen from this figure that the obtained highest efficiency reaches $\eta = 11.12\%$. The associated electrical characteristics of the solar cell are as follows:

- open circuit voltage: $V_{oc} = 0.374\ V$,
- short circuit current density: $J_{sc} = 39.09\ mA/cm^2$
- fill factor: $FF = 75.99\%$.

Quadratic polynomial regression which was performed on the obtained results has enabled to derive the following response surface model for the solar cell efficiency:

$$\eta(\%) = 9.97794 + 1.56775\times10^{-21}W_d + 2.68183\times10^{-19}B_d + 2.8115\times10^{-40}W_d\times B_d - 1.1067\times10^{-42}Wd^2 - 6.7067\times10^{-38}Bd^2 \quad (10)$$

One can notice from Eq. (10) that efficiency increases with Window doping. So, theoretically further enhancement of the optimum found here could be attained. However, this should be considered by taking carefully into account the other parameters. The physical models should also be adapted as some antagonist effect may exist between factors. This fact cannot be anticipated by using simply the same physical models than those employed here, for which Eq. (10) holds, and which were validated by considering the ranges of design variables based on the experimental results given in [11]. Further investigation is then needed.

Table 5. Levels of the parameters considered in the third series of simulations. (Own source)

Factor	$Wd(cm^{-3})$	$Bd(cm^{-3})$
Low level	4×10^{20}	10^{18}
Intermediate level	5×10^{20}	1.5×10^{18}
High level	6×10^{20}	2×10^{18}

3.4. The optimized structure

Figures 6 and 7 depict the obtained optimal design of the single-junction solar cell structure, which is based on GaSb semiconductor material having window and BSF thin layers made from $Al_{0.5}Ga_{0.5}As_{0.96}Sb_{0.96}$ material. This corresponds to the solution as obtained by executing the optimization procedure which was detailed in the previous sections.

For the conditions of illumination of one-Sun AM1.5 G solar spectrum and the ambient temperature of 300°K, the current density-voltage characteristic (J−V curve) of the improved design of the studied structure of solar cell is plotted in Fig. 8.

To assess the added value of the improved single-junction solar cell found in the present work, a comparison is performed between its electrical characteristics and those published in previous research. These consisted of simulated devices as well as experimental work. Table 6 summarizes the photovoltaic performances of the actual optimal design with those taken from literature.

One can see that the optimal design set up in the present work shows enhanced performance with up-to-date known other results. However, this is theoretical and experimental verification of this finding is needed in order to authenticate its feasibility in practice.

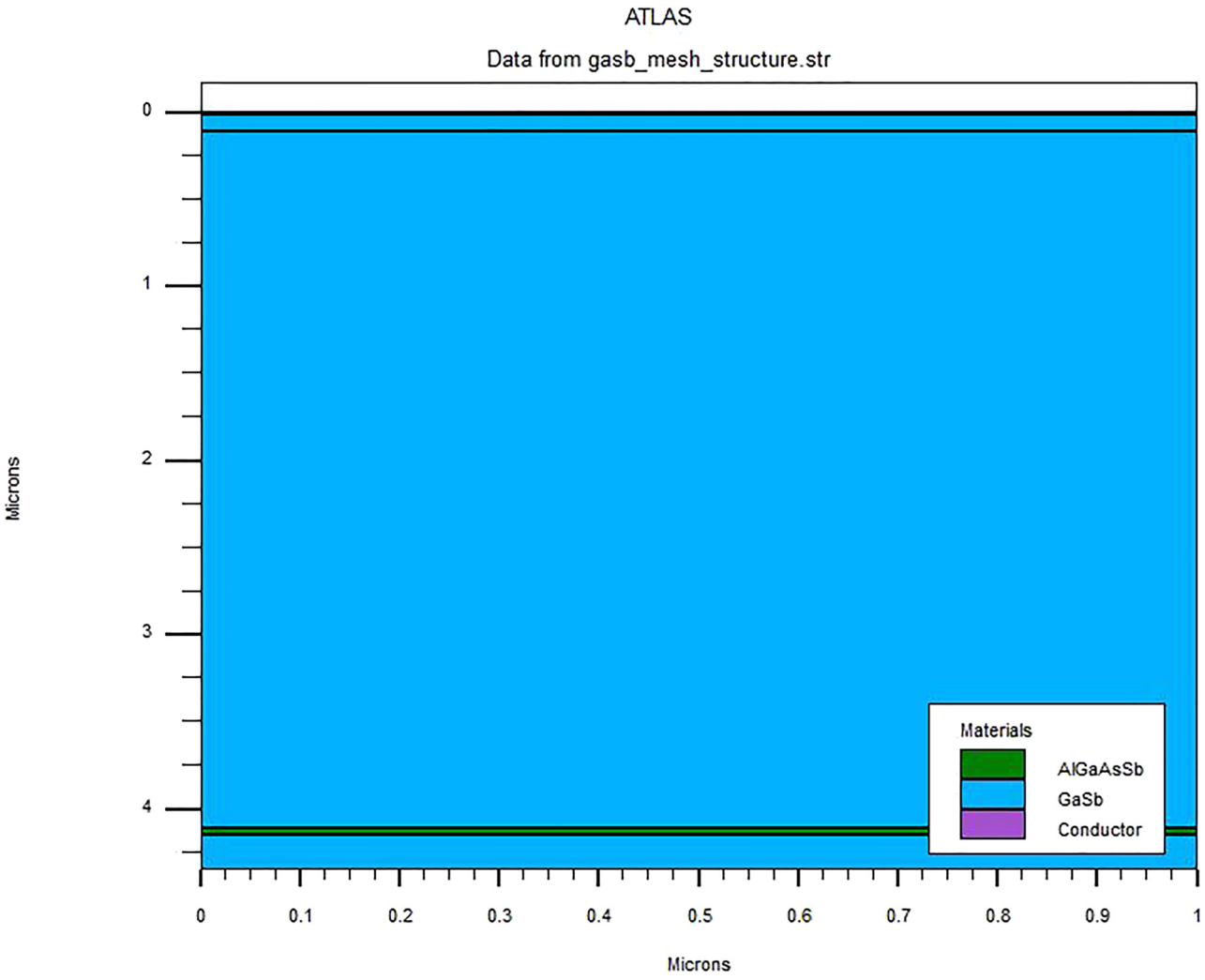

Fig. 6. Design structure of the optimized GaSb cell design. (Own source)

Window	$Al_{0.5}Ga_{0.5}As_{0.04}Sb_{0.96}$	$W_{dn} = 6.10^{20}cm^{-3}$	$W_t = 0.01\mu m$
Emitter	GaSb	$E_{dn} = 5.10^{17}cm^{-3}$	$E_t = 0.1\mu m$
Base	GaSb	$B_{dp} = 2.10^{18}cm^{-3}$	$B_t = 4\mu m$
BSF	$Al_{0.5}Ga_{0.5}As_{0.04}Sb_{0.96}$	$BSF_{dn} = 1.510^{19}cm^{-3}$	$BSF_t = 0.035\mu m$
Buffer	GaSb	$Buf_{dn} = 1.510^{18}cm^{-3}$	$Buf_t = 0.2\mu m$
Substrate	GaSb	$Sub_{dn} = 7.10^{17}cm^{-3}$	

Fig. 7. Schematic structure of the optimal structure of the GaSb single junction solar cell. (Own source)

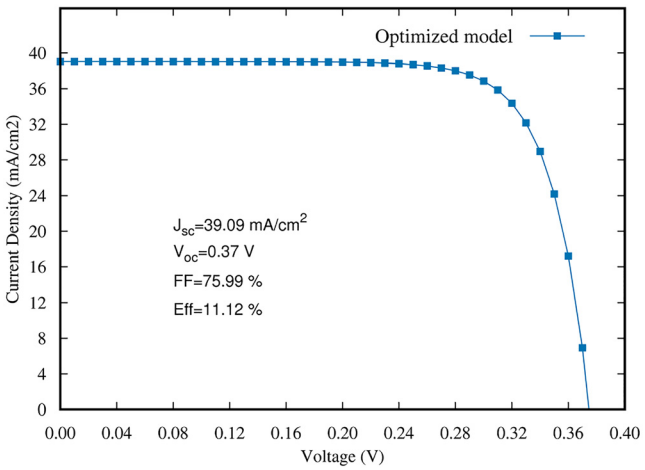

Fig. 8. The characteristic J-V curve for the optimized structure of the studied GaSb based single junction solar cell. (Own source)

Table 6. Comparison of the performance of the optimized structure obtained in the present work with previously published works on GaSb single junction solar cells. (Own source)

Reference	V_{oc} in V	J_{sc} in mA/cm^2	FF in %	Efficiency in %
[18]	0.23	19.21	67	3
[19]	0.27	32	52	4.4
[11]	0.312	38.8	59.6	7.26
This work	0.374	39.09	75.99	11.12

4. CONCLUSIONS

Single-junction solar cells made of GaSb material and having AlGaAsSb window and back surface field layers were studied numerically by means of SILVACO-ATLAS software. Simulations were conducted by varying key design variables in order to determine at first the most dominant factors with regards to efficiency. It has been found that, in the considered ranges of parameters, Window doping and Base doping affect predominantly the GaSb cell performance. A three step optimization procedure was proposed and has enabled to reach an optimal design, for which the obtained cell exhibited improved photovoltaic performance with $V_{oc} = 0.374\ V$, $J_{sc} = 39.09\ mA/cm^2$, $FF = 75.99\%$ and optimal conversion efficiency attaining $\eta = 11.12\%$. Comparison with previous works demonstrated that the optimized solar cell shows better efficiency. The simulation aided optimization procedure introduced here is general. It has the advantage to offer a systematic guideline for designing and fabricating improved solar cells. However, the significance of the obtained results is supported by the physical models used in simulations. These are relative to the particular structure of the studied solar cell and were validated for parameters rangers which remain in the vicinity of those tested experimentally for the same solar cell configuration. Any generalization of the methodology used should consider adequacy of the physical models to be used. Finally, experimental verification of the findings of this work is still needed in order to assess definitely their practical usefulness.

REFERENCES

[1] J. Jang, J. Song, S.S. Lee, S. Jeong, B. J. Lee, and S. Kim, "Analysis of temperature-dependent I-V characteristics of the Au/n-GaSb Schottky diode," *Mater. Sci. Semicond. Process.*, vol. 131, p.105882, 2021. https://doi.org/10.1016/j.mssp.2021.105882.

[2] E. B. Elkenany, "Theoretical investigations of electronic, optical and mechanical properties for GaSb and AlSb semiconductors under the influence of temperature," *Spectrochimica Acta Part A: Mol. Biomol. Spectrosc.*, vol. 150, pp. 15–20, 2015. https://doi.org/10.1016/j.saa.2015.05.033.

[3] L. M. Fraas, J. E. Avery, and H. X. Huang, "Thermophotovoltaics: Heat and electric power from low bandgap" solar" cells around gas fired radiant tube burners," *Conference Record of the Twenty-Ninth IEEE Photovoltaic Specialists Conference*, pp. 1553–6, 2002. https://doi.org/10.1109/pvsc.2002.1190909.

[4] L. Fraas, J. Avery, R. Ballantyne, and W. Daniels, "GaSb photovoltaic cells ready for space and the home," *III-Vs Rev.*, vol. 12, no.4, pp. 22–6, 1999. https://doi.org/10.1016/s0961-1290(99)80076-3.

[5] A. W. Bett, S. Keser, G. Stollwerck, O. V. Sulima, and W. Wettling, "Over 31%-efficient GaAs/GaSb tandem concentrator solar cells," *Conference Record of the Twenty Sixth IEEE Photovoltaic Specialists Conference*, 1997. https://doi.org/10.1109/pvsc.1997.654240.

[6] G. S. Sahoo and G. P. Mishra, "Effective use of spectrum by an ARC less dual junction solar cell to achieve higher efficiency: a simulation study," *Superlattices and Microstruct.*, vol. 109, pp. 794–804, 2017. https://doi.org/10.1016/j.spmi.2017.06.002.

[7] C. A. Wang, "Progress and continuing challenges in GaSb-based III–V alloys and heterostructures grown by organometallic vapor-phase epitaxy," *J. Cryst. Growth*, vol. 272, no.1–4, pp. 664–81, 2004. https://doi.org/10.1016/j.jcrysgro.2004.09.019.

[8] F. Dimroth, T. N. D. Tibbits, M. Niemeyer, F. Predan, P. Beutel, C. Karcher, E. Oliva, G. Siefer, D. Lackner, P. Fuß-Kailuweit, A. W. Bett, R. Krause, C. Drazek, E. Guiot, J. Wasselin, A. Tauzin, and T. Signamarcheix, "Four-junction wafer-bonded concentrator solar cells," *IEEE J. Photovoltaics*, vol. 6, no. 1, pp. 343–9, 2016. https://doi.org/10.1109/jphotov.2015.2501729.

[9] M. P. Lumb, M. Meitl, K. J. Schmieder, M. Gonzalez, S. Mack, M.K. Yakes, and R.J. Walters, "Towards the ultimate multi-junction solar cell using transfer printing," *43rd Photovoltaic Specialists Conference (PVSC)*, pp. 0040–5, 2016.

[10] F. Predan, D. Lackner, E. Oliva, A. Kovács, W. Jäger, and F. Dimroth, "Developments for wafer-bonded four-junction solar cells based on GaSb," *7th World Conference on Photovoltaic Energy Conversion (WCPEC)*, pp. 1–6, 2018.

[11] S. Parola, A. Vauthelin, J. Tournet, J. Kret, J. El Husseini, F. Martinez, Y. Cuminal, "Improved efficiency of GaSb solar cells using an Al0.50Ga0.50As0.04Sb0.96 window layer," *Solar Energy Mater. Solar Cells*, vol. 200, pp. 110042, 2019. https://doi.org/10.1016/j.solmat.2019.110042.

[12] S. Adachi, "Band gaps and refractive indices of AlGaAsSb, GaInAsSb, and InPAsSb: key properties for a variety of the 2–4-μm optoelectronic device applications," *J. Appl. Phys.*, vol. 61, no. 10, pp. 4869–76, 1987. https://doi.org/10.1063/1.338352.

[13] S. K. Saha, "Modelling the effectiveness of computer-aided development projects in the semiconductor industry," *Int. J. Eng. Manag. Econ.*, vol. 1, nos. 2–3, pp. 162–78, 2010. https://doi.org/10.1504/ijeme.2010.036948.

[14] A. K. Goel, M. Merry, K. Arkenberg, E. Therkildsen, E. Chiaburu, and W. Standfest, "Optimization of device performance using semiconductor TCAD tools," Tech. Rep., Santa Clara, CA, USA, 2001.

[15] I. Silvaco, *ATLAS User's Manual Device Simulation Software*. Santa Clara, CA, USA, 2010.

[16] K. Weiwei, TCAD Simulation and Modeling of AlGaN/GaN HFETs. Doctoral dissertation, Ph.D. thesis, Faculty of North Carolina State University, USA, 2011.

[17] N. Papež, R. Dallaev, Ş. Ţălu, and J. Kaštyl, "Overview of the current state of gallium Arsenide-based solar cells," *Materials*, vol. 14, no. 11, pp. 3075, 2021. https://doi.org/10.3390/ma14113075.

[18] F. Z. Meharrar, A. Belfar, I. Aouad, E. Giudicelli, Y. Cuminal, and H. Aït-Kaci, "Analysis of the GaSb-p+/GaSb-p/GaSb-n+/GaSb-n structure performances at room temperature for thermo-photovoltaic applications," *Optik*, vol. 175, pp. 138–47, 2018.

[19] J. Tournet, S. Parola, A. Vauthelin, D. Montesdeoca Cardenes, S. Soresi, F. Martinez, and E. Tournié, "GaSb-based solar cells for multi-junction integration on Si substrates," *Solar Energy Mater. Solar Cells*, vol. 191, pp. 444–50, 2019. https://doi.org/10.1016/j.solmat.2018.11.035.